Porous Silicon Nanoparticles with Rare Earth as Potential Contrast Agents for MRI and Luminescent Probes for Bioimaging

Anastasiya D. Mironova[1*], Yulia V. Kargina[1,2], Olga S. Pavlova[2,3], Alexander M. Perepukhov[4], Igor O. Sobina[2], and Victor Yu. Timoshenko[1,2]

[1] Phys-Bio Institute, National Research Nuclear University "MEPhI", 31 Kashirskoe shosse, Moscow 115409, Russia
[2] Faculty of Physics, Lomonosov Moscow State University, 1 Leninskie Gory, Moscow 119991, Russia
[3] Faculty of Fundamental Medicine, Lomonosov Moscow State University, 1 Leninskie Gory, Moscow 119991, Russia
[4] Institute of Physics and Technology, 9 Institutskiy per., Dolgoprudny 141700, Moscow Region, Russia

*** e-mail:** navonorim@mail.ru

Abstract. Nanoparticles of porous silicon with incorporated europium and gadolinium ions were prepared by using mechanical grinding of electrochemically grown mesoporous silicon films followed with impregnation with rare earth ions from aqueous solutions. The photoluminescence spectroscopy of europium doped porous silicon nanoparticles allowed us to reveal narrow lines associated with the $^5D_0 \rightarrow {}^7F_4$ transitions in Eu^{3+} ions. Measurements of the proton relaxation in aqueous suspensions of nanoparticles with embedded Gd^{3+} ions showed an effect of the shortening of both the longitudinal and transverse relaxation times. Potential applications of rare earth doped porous silicon nanoparticles as contrast agents in MRI and fluorescent labels in bioimaging are discussed.

Keywords: nanoparticles; aqueous suspensions; proton relaxation; magnetic resonance imaging; contrast agent.

Paper #3477 received 19 Feb 2022; revised manuscript received 4 Apr 2022; accepted for publication 1 May 2022; published online 18 May 2022. doi: 10.18287/JBPE22.08.020304.

1 Introduction

Magnetic resonance imaging (MRI) is widely used in medical practice because this diagnostic method is safe and has a high spatial resolution [1]. Molecular substances called contrast agents (CAs) can significantly enhance the MRI contrast [2, 3]. Novel CAs based on nanoparticles (NPs) are being studied and developed [4]. Most clinically approved types of CAs consist of ions of gadolinium (Gd) [5–7] and iron (Fe) [8, 9]. Recently new types of CAs based on silicon (Si) NPs have been proposed [10, 11]. It was shown that CA properties of Si NPs could be significantly improved after incorporation of Fe^{3+} [12]. However, Gd-based substances are one of the most common CAs for clinical diagnostic purposes. They have a high relaxivity and increase the signal intensity due to a decrease in the longitudinal relaxation that is explained by the interaction of proton spins of water molecules with electron spins of rare earth ions [3, 13–15]. The disadvantage is the toxicity of free Gd^{3+} ions, which can cause allergic reactions in some patients. To reduce the toxic effect of free Gd^{3+} ions, it is proposed to bind them with biocompatible Si NPs and reduce the concentration of ions in the CA. It is important that the CA remains effective. Besides Gd^{3+}, trivalent ions Eu^{3+} are considered as potential labels in biomedical diagnostics [16]. The aim of our work is to study the effect of incorporated Gd^{3+} and Eu^{3+} ions in porous Si NPs on the proton relaxation in aqueous solutions as well the photoluminescence property rare earth doped MPSi NPs as possible CAs for MRI and probes for fluorescent bioimaging.

2 Materials and Methods

Aqueous suspensions of mesoporous Si (MPSi) NPs were prepared by electrochemical etching of crystalline Si (c-Si) wafers followed by mechanical grinding of the formed mesoporous films in water by using a planetary mill [10]. To obtain a uniform distribution of MPSi NPs

in water, all samples were exposed to ultrasound for 30 min. Then, suspensions of MPSi NPs with concentration about 10 mg/mL were mixed with aqueous solutions of lanthanide chlorides ($EuCl_3$ and $GdCl_3$) at different concentrations of the latter varied from 10 to 50 mg/mL. The prepared mixtures were stored for 30 min followed with centrifugation and cleaning by deionized water two times to remove unbound lanthanide ions. Then the samples were diluted to obtain aqueous suspensions of MPSi:Gd and MPSi:Eu NPs with concentration of the order of 1 mg/mL.

The hydrodynamic diameter and surface charge (zeta-potential) of the MPSi NPs were estimated by using a methods of the dynamic light scattering (DLS) with a ZetasizerNano Malvern DLS spectrometer (Malvern Instruments, United Kingdom). A part of the prepared aqueous suspensions was dried at room temperature in air to analyze their chemical composition by means of the X-ray fluorescence (XRF) spectroscopy using a Renom apparatus (Expert Center Ltd., Russia). Photoluminescence (PL) spectra of MPSi NPs and those with Eu^{3+} ions under excitation with a semiconductor laser at 465 nm were measured by using a grating monochromator equipped with a CCD unit (Mightex, Canada). To measure the proton relaxation times in aqueous suspensions of MPSi NPs we used a Bruker Minispec NMR relaxometer (Bruker, Germany) with a constant magnetic field strength of about 0.5 T. The relaxation times were measured for 800 μL of aqueous suspensions of NPs in glass ampoules placed in a thermostat at 40 °C.

3 Results and Discussion

DLS measurements reveal that prepared MPSi NPs are characterized by hydrodynamic diameter and zeta-potential of about 560 nm and –6 mV, respectively. The negative value of the latter indicates the predominant role of hydroxyl groups on the surface of MPSi NPs [10]. The initial negative charge of NPs can obviously promote the electrostatic binding between the NP's surface and positively charged lanthanide ions, i.e. Gd^{3+} and Eu^{3+} in aqueous solutions.

Fig. 1 shows typical XRF spectra of MPSi NPs with incorporated rare earth and reference samples of dried lanthanide chlorides and initial MPSi NPs. The characteristic X-ray emission lines of the L-series in Europium at 5.82-5.85, 6.46, 6.84 and 7.48 keV [17] are detected for $EuCl_3$ and MPSi:Eu NPs (see Fig. 1a). The characteristic L-shell lines of the Gadolinium at 6.03–6.06, 6.71, 7.10, and 7.79 keV [17] are also detected in MPSi:Gd NPs prepared at the initial rare earth concentration about 10 mg/mL (see Fig 2b). By comparing with the XRF line intensities the europium concentration in MPSi:Eu are estimated to be about 48.7 at.% that indicates a high efficiency of the incorporation of Eu^{3+} ions into MPSi NPs. This fact can be explained by high internal surface area and negative surface charge of the latter [18]. The Gd content is about 0.09 and 0.33 at.% in MPSi NPs samples prepared at the $GdCl_3$ concentration of 10 mg/mL and 50 mg/mL, respectively. The smaller relative content of rare earth in MPSi:Gd NPs in comparison with that in MPSi:Eu ones can be related to different efficiency of the incorporation into oxidized internal surface of MPSi. Table 1 presents XRF data on the rare earth concentration in the samples under study.

Table 1 Rare earth content in MPSi NPs according to XRF data.

Sample	Rare earth content, at.%
MPSi:Eu (46mg/mL)	48.70
MPSi:Gd (50 mg/mL)	0.33
MPSi:Gd (10 mg/mL)	0.09

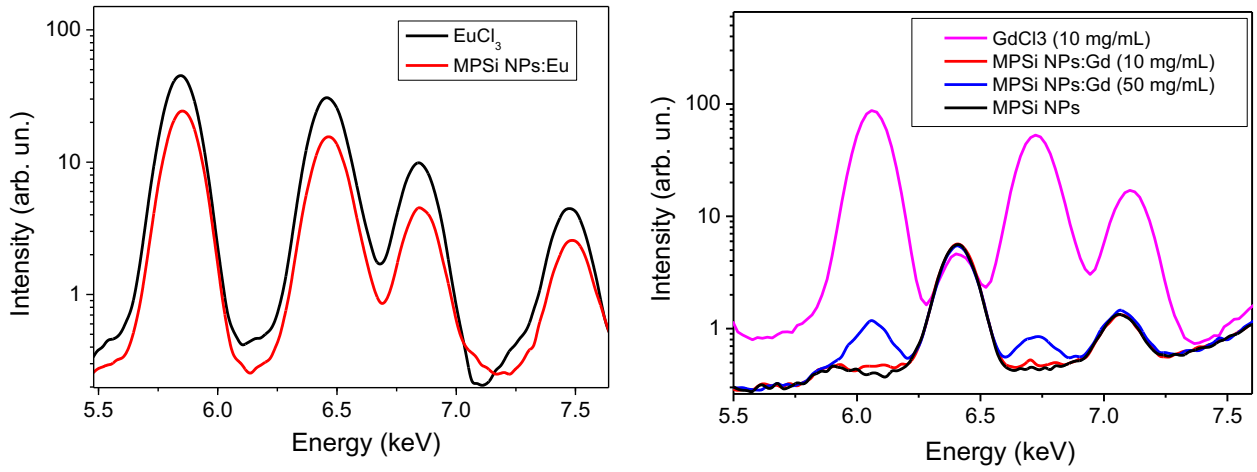

(a) (b)

Fig. 1 XRF spectra of the following samples: (a) $EuCl_3$ (46 mg/mL) and MPSi NPs with Eu^{3+} ions incorporated from aqueous solution with the same rare earth concentration; (b) $GdCl_3$ (10 mg/mL), MPSi NPs with Gd^{3+} ions incorporated from aqueous solutions at different concentrations and pure MPSi NPs.

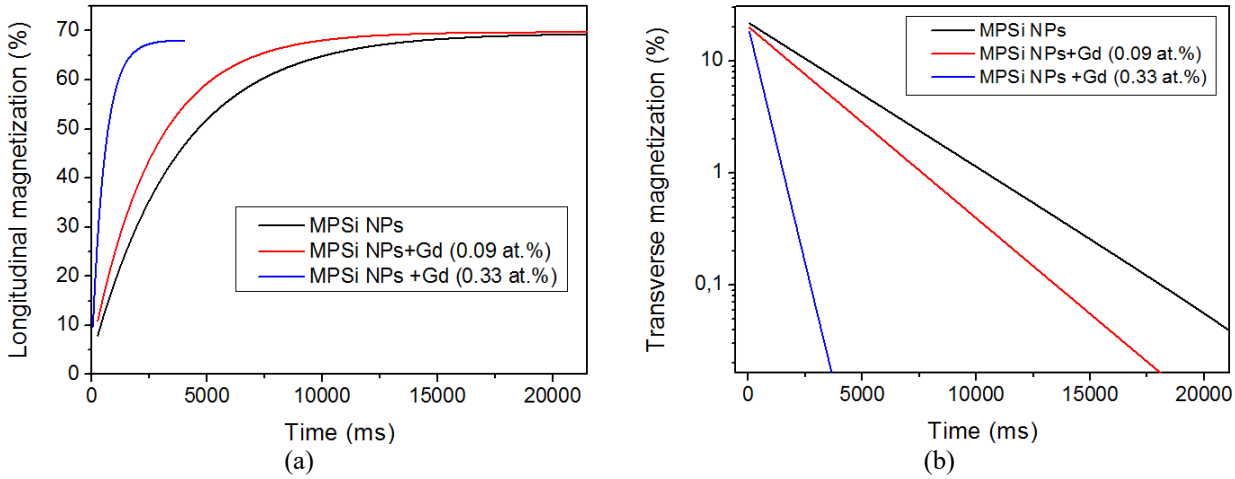

Fig. 2 Transients of the longitudinal (a) and transverse (b) components of the proton magnetization for aqueous suspensions of MPSi NPs and those with incorporated Gd^{3+} ions with different concentration.

Fig. 2 shows transients of the longitudinal and transverse components of the proton magnetization for suspensions of MPSi:Gd NPs. While pure MPSi NPs do not significantly affect the proton relaxation, Gd^{3+} ions introduced into the NPs lead to a shortening of both the longitudinal and transverse relaxation times. Table 2 summarizes the times of longitudinal and transverse proton relaxation for pure MPSi NPs and those with incorporated rare earth ions. It is seen that MPSi:Eu NPs are not effective CA for MRI because of the well-known low relaxivity efficiency of Eu^{3+} ions, in contrast to MPSi NPs with Gd^{3+} ions, which decrease the relaxation times by 3 orders of magnitude.

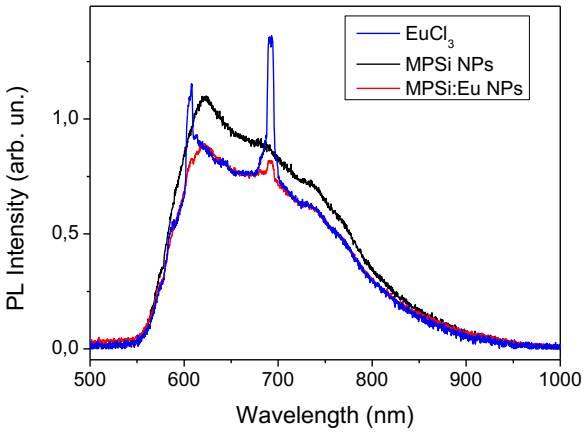

Fig. 3 PL spectra of aqueous solution of $EuCl_3$, suspensions of MPSi and MPSi:Eu NPs.

Fig. 3 shows PL spectra of MPSi:Eu NPs, $EuCl_3$, and pure MPSi NPs. The spectra of $EuCl_3$ and MPSi NPs with incorporated Eu^{3+} ions exhibit characteristic narrow lines associated with the $^5D_0 \rightarrow {}^7F_4$ transition in Eu^{3+} [16, 19]. The broad PL band in the region from 550 nm to 900 nm can be related to the radiative emission processes in the hydroxide layer of MPSi NPs [18] as well as in optically excited Eu^{2+}ions [19]. It is interesting to note that in our experiments the Eu^{3+}PL is efficiently excited by the green-blue light with wavelength of 465 nm, which corresponds to relatively weak absorption due to the $^7F_0 \rightarrow {}^5D_2$ transition in Eu^{3+}[19]. The possibility to excite MPSi:Eu NPs by visible light seems to be useful for bioimaging application [16].

Table 2 Data on the longitudinal (T_1) and transverse (T_2) relaxation times for aqueous suspensions of MPSi NPs without and with rare earth incorporation as well for the corresponding lanthanide salts and water for comparison.

Sample	**T_1 (ms)**	**T_2 (ms)**
Water	4360 ± 10	3500 ± 10
MPSi, 1 mg/mL	3784 ± 10	3452 ± 10
$EuCl_3$, 46 mg/mL	2297 ± 10	2012 ± 10
$GdCl_3$, 1 mg/mL	3.2 ± 0.6	2.77 ± 0.06
MPSi:Gd (0.09 at. %), 1 mg/mL	2769 ± 10	2540 ± 10
MPSi:Gd (0.33 at. %), 1 mg/mL	565 ± 5	514 ± 5

4 Conclusions

Aqueous suspensions of mesoporous Si NPs with incorporated Eu^{3+} and Gd^{3+} ions are prepared by using mechanical grinding of the electrochemically grown mesoporous silicon films followed with impregnation by the rare earth in concentrated aqueous solutions of the corresponding lanthanide chlorides. It is established that Gd^{3+} ions incorporated into MPSi NPs even at low concentration about 0.33 at.% can significantly decrease both the longitudinal and transverse times of the proton relaxation in water molecules in aqueous media. This observation opens new possibilities for Gd-doped MPSi NPs as potential CA in biomedical MRI diagnostics. The good degree of binding and characteristic PL emission in the visible spectral range of Eu^{3+} ions are found for MPSi

NPs impregnated with rare earth in $EuCl_3$ solutions. This optical property can be of interest for applications of Eu-doped MPSi NPs, for example, as fluorescent probes in bioimaging.

Disclosures

The authors have no relevant financial interests in this article and no potential conflicts of interest to disclose.

References

1. J. C. Weinreb, H. C. Redman, "Musculoskeletal System," Chapter 12 in Magnetic Resonance Imaging of the Body: Advanced Exercises in Diagnostic Radiology Series, J. C. Weinreb, H. C. Redman, Saunders, Philadelphia, 214–259 (1987).
2. S. Aime, A. Barge, C. Cabella, S. G. Crich, and E. Gianolio, "Targeting cells with MR imaging probes based on paramagnetic Gd(III) chelates," Current Pharmaceutical Biotechnology 5(6), 509–518 (2004).
3. A. Y. Louie, M. M. Hüber, E. T. Ahrens, U. Rothbächer, R. Moats, R. E. Jacobs, S. E. Fraser, and T. J. Meade, "In vivo visualization of gene expression using magnetic resonance imaging," Nature Biotechnology 18, 321–325 (2000).
4. O. Salata, "Applications of nanoparticles in biology and medicine", Journal of Nanobiotechnology 2, 3 (2004).
5. P.-J. Debouttière, S. Roux, F. Vocanson, C. Billotey, O. Beuf, A. Favre-Réguillon, Y. Lin, S. Pellet-Rostaing, R. Lamartine, P. Perriat, and O. Tillement, "Design of Gold Nanoparticles for Magnetic Resonance Imaging," Advanced Functional Materials 16(18), 2330–2339 (2006).
6. F. Lux, V. L. Tran, E. Thomas et al., "AGuIX® from bench to bedside—Transfer of an ultrasmall theranostic gadolinium-based nanoparticle to clinical medicine," The British Journal of Radiology 92(1093), 20180365 (2018).
7. J. Morlieras, S. Dufort, L. Sancey, C. Truillet, A. Mignot, F. Rossetti, M. Dentamaro, S. Laurent, L. V. Elst, R. N. Muller, R. Antoine, P. Dugourd, S. Roux, P. Perriat, F. Lux, J.-L. Coll, and O. Tillement, "Functionalization of small rigid platforms with cyclic RGD peptides for targeting tumors overexpressing αvβ3 integrins," Bioconjugate Chemistry 24(9), 1584–1597 (2013).
8. K. Ishiyama, S. Motoyama, N. Tomura, R. Sashi, H. Imano, J.-I. Ogawa, K. Narita, and J. Watarai, "Visualization of lymphatic basin from the tumor using magnetic resonance lymphography with superparamagnetic iron oxide in patients with thoracic esophageal cancer," Journal of Computer Assisted Tomography 30(2), 270–275 (2006).
9. A. Tanimoto, S. Kuribayashi, "Application of superparamagnetic iron oxide to imaging of hepatocellular carcinoma," European Journal of Radiology 58(2), 200–216 (2006).
10. Y. V. Kargina, M. B. Gongalsky, A. M. Perepukhov, A. A. Gippius, A. A. Minnekhanov, E. A. Zvereva, A. V. Maximychev, and V. Yu. Timoshenko, "Investigation of proton spin relaxation in water with dispersed silicon nanoparticles for potential magnetic resonance imaging applications," Journal of Applied Physics 123(10), 104302 (2018).
11. Y. V. Kargina, A. M. Perepukhov, A. Yu. Kharin, E. A. Zvereva, A. V. Koshelev, S. V. Zinovyev, A. V. Maximychev, A. F. Alykova, N. V. Sharonova, V. P. Zubov, M. V. Gulyaev, Y. A. Pirogov, A. N. Vasiliev, A. A. Ischenko, and V. Yu. Timoshenko, "Silicon nanoparticles prepared by plasma-assisted ablative synthesis: physical properties and potential biomedical applications," Physica Status Solidi (A) 216(14), 1800897 (2019).
12. Y. V. Kargina, S. V. Zinovyev, A. M. Perepukhov, E. V. Suslova, A. A. Ischenko, and V. Yu. Timoshenko, "Silicon nanoparticles with iron impurities for multifunctional applications," Functional Materials Letters 13(4), 2040007 (2020).
13. K. N. Raymond, V. C. Pierre, "Next generation, high relaxivity gadolinium MRI agents," Bioconjugate Chemistry 16(1), 3–8 (2005).
14. Z. Wang, F. Carniato, Y. Xie, Y. Huang, Y. Li, S. He, N. Zang, J. D. Rinehart, M. Botta, and N. C. Gianneschi, "High relaxivity gadolinium-polydopamine nanoparticles," Small 13(43), 1701830 (2017).
15. M. Engström, A. Klasson, H. Pedersen, C. Vahlberg, P.-O. Käll, and K. Uvdal, "High proton relaxivity for gadolinium oxide nanoparticles," Magnetic Resonance Materials in Physics, Biology and Medicine 19(4), 180–186 (2006).
16. M. Donmez, H. A. Oktem, and M. D. Yilmaz, "Ratiometric fluorescence detection of an anthrax biomarker with Eu^{3+}-chelated chitosan biopolymers," Carbohydrate Polymers 180, 226–230 (2018).
17. J. A. Bearden, "X-Ray Wavelengths," Reviews of Modern Physics 39(1), 78–124 (1967).
18. A. S. Eremina, Y. Kargina, A. Y. Kharin, D. I. Petukhov, and V. Y. Timoshenko, "Mesoporous silicon nanoparticles covered with PEG molecules by mechanical grinding in aqueous suspensions," Microporous and Mesoporous Materials 331, 111641 (2022).
19. I. N. Ogorodnikov, V. A. Pustovarov, "Linear optical, luminescence and electronic properties of the La2Be2O5 laser crystals doped with Ce3+ or Eu3+," Journal of Luminescence 162, 50–57 (2015).